Supplemental Materials to the article:

Dimensional quantization and waveguide effect of Dyakonov surface waves in twisted confined media

D. A. Chermoshentsev[1,2,3], E. V. Anikin[1], S. A. Dyakov[1], and N. A. Gippius[1]

[1]Skolkovo Institute of Science and Technology, Moscow 143025, Russia
[2]Moscow Institute of Physics and Technology, Moscow Region 141701, Russia
[3]Russian Quantum Center, Skolkovo, Moscow 143026 , Russia

September 15, 2020

1 Interface of two uniaxial crystals

At $z > 0$ optical axis is x, and the solutions for ordinary and extraordinary waves take form

$$\vec{E}_o^+ = \frac{1}{k_0}\begin{pmatrix} 0 \\ -k_z^{o+} \\ k_y \end{pmatrix} e^{i\vec{k}\vec{r}}, \quad \vec{B}_o^+ = \frac{1}{k_0^2}\begin{pmatrix} k_0^2\epsilon_1 - k_x^2 \\ -k_x k_y \\ -k_x k_z^{o+} \end{pmatrix} e^{i\vec{k}\vec{r}} \tag{1}$$

$$\vec{E}_e^+ = \frac{1}{k_0^2}\begin{pmatrix} -k_0^2\epsilon_1 + k_x^2 \\ k_x k_y \\ k_z^{e+} k_x \end{pmatrix} e^{i\vec{k}\vec{r}}, \tag{2}$$

$$\vec{B}_e^+ = \frac{1}{k_0}\begin{pmatrix} 0 \\ -\epsilon_1 k_z^{e+} \\ \epsilon_1 k_y \end{pmatrix} e^{i\vec{k}\vec{r}}, \tag{3}$$

$$\begin{gathered} k_z^{o+} = \sqrt{k_0^2\epsilon_1 - k_x^2 - k_y^2}, \\ k_z^{e+} = \sqrt{k_0^2\epsilon_2 - \gamma k_x^2 - k_y^2}, \\ \gamma = \epsilon_2/\epsilon_1. \end{gathered} \tag{4}$$

At $z < 0$ optical axis is y, and

$$\vec{E}_o^- = \frac{1}{k_0}\begin{pmatrix} k_z^{o-} \\ 0 \\ -k_x \end{pmatrix} e^{i\vec{k}\vec{r}}, \quad \vec{B}_o^- = \frac{1}{k_0^2}\begin{pmatrix} -k_x k_y \\ k_0^2\epsilon_1 - k_y^2 \\ -k_y k_z^{o-} \end{pmatrix} e^{i\vec{k}\vec{r}} \tag{5}$$

$$\vec{E}_e^- = \frac{1}{k_0^2}\begin{pmatrix} k_x k_y \\ -k_0^2\epsilon_1 + k_y^2 \\ k_y k_z^{e-} \end{pmatrix} e^{i\vec{k}\vec{r}}, \tag{6}$$

$$\vec{B}_e^- = \frac{1}{k_0}\begin{pmatrix} \epsilon_1 k_z^{e-} \\ 0 \\ -\epsilon_1 k_x \end{pmatrix} e^{i\vec{k}\vec{r}}, \tag{7}$$

$$\begin{gathered} k_z^{o-} = \sqrt{k_0^2\epsilon_1 - k_x^2 - k_y^2} \\ k_z^{e-} = \sqrt{k_0^2\epsilon_2 - k_x^2 - \gamma k_y^2} \end{gathered} \tag{8}$$

Note that $k_z^{o\pm,e\pm}$ should be imaginary in order to the solution be localized at the interface. The wavevectors k_z^{o+}, k_z^{e+} (k_z^{o-}, k_z^{e-}) should have positive (negative) imaginary part.

Explicitly the dispersion equation (Section II, Eq (2)) can be written in the following form:

$$\begin{aligned} k_0^2\epsilon_1(k_z^{o+})^2(k_z^{o-})^2 - (k_0^2\epsilon_1 - k_x^2)(k_0^2\epsilon_1 - k_y^2)(k_z^{o+}k_z^{e-} + k_z^{e+}k_z^{o-}) + \\ + k_0^2\epsilon_1 k_z^{o-}k_z^{o+}k_z^{e-}k_z^{e+} + (k_z^{o-}k_z^{e-} + k_z^{o+}k_z^{e+})k_x^2k_y^2 = 0 \end{aligned} \tag{9}$$

2 One-dimensional confinement at $\alpha = 0°$

As our interface of two anisotropic crystals has the following mirror symmetries $x \to -x$ and $y \to -y$ it is possible to treat the reflectance from ideally conducting mirror at $x = const$ or $y = const$. In such case we consider the DW which is propagates along x-axis with $k_y = 0$. If the plane wave solution is known $\vec{E}_{k_x} = \vec{E}_{k_x}(y,z)e^{ik_x x}$ that the solution satisfied mirror boundary condition at $x = 0$ has the following form:

$$\vec{E}^{\text{tot}}(x,y,z) = \vec{E}_{k_x}(y,z)e^{ik_x x} - \vec{E}_{-k_x}(y,z)e^{-ik_x x} \tag{10}$$

Due to the geometry of the interface this solution also should satisfy mirror boundary condition at $x = d$, which leads to $k_x d = \pi n$, where $n \in \mathbb{N}$. In case of ideal reflectance without scattering losses, the k_x for DW can be calculated from Eq. (6). Finally, the dispersion law of DW get the following form:

$$k_x d = \beta(k_0, \pi/4)d = \pi n \tag{11}$$

which means that for the fixed wavelength the DW can exist only in the discrete set of distances between boundaries d. The calculated dispersion curves depending on the anisotropy factor of the permittivities ϵ_2/ϵ_1 are shown in Fig. 1c. We have stimulated the Fabry-Perot resonance for the Dyakonov mode with $\lambda = 1550$ nm in the case of reflection from the anisotropic crystals - air interface and $n = 10$ (Fig. 1c red dot). The permittivity tensor $\epsilon_1 = 9$ and $\epsilon_2 = 16$ was selected. The obtained results is close to our theoretical results from Eq. (11). The distributions of the intensities of the electric and magnetic fields in this mode are presented in Fig. 1d-e. As one can see from the Fig. 1d, most of the energy in mode is lost due to passing through the reflecting boundary, so such resonances are not have a high quality-factor. The Q-factor calculated for this resonance is equal to $Q = 26.1$.

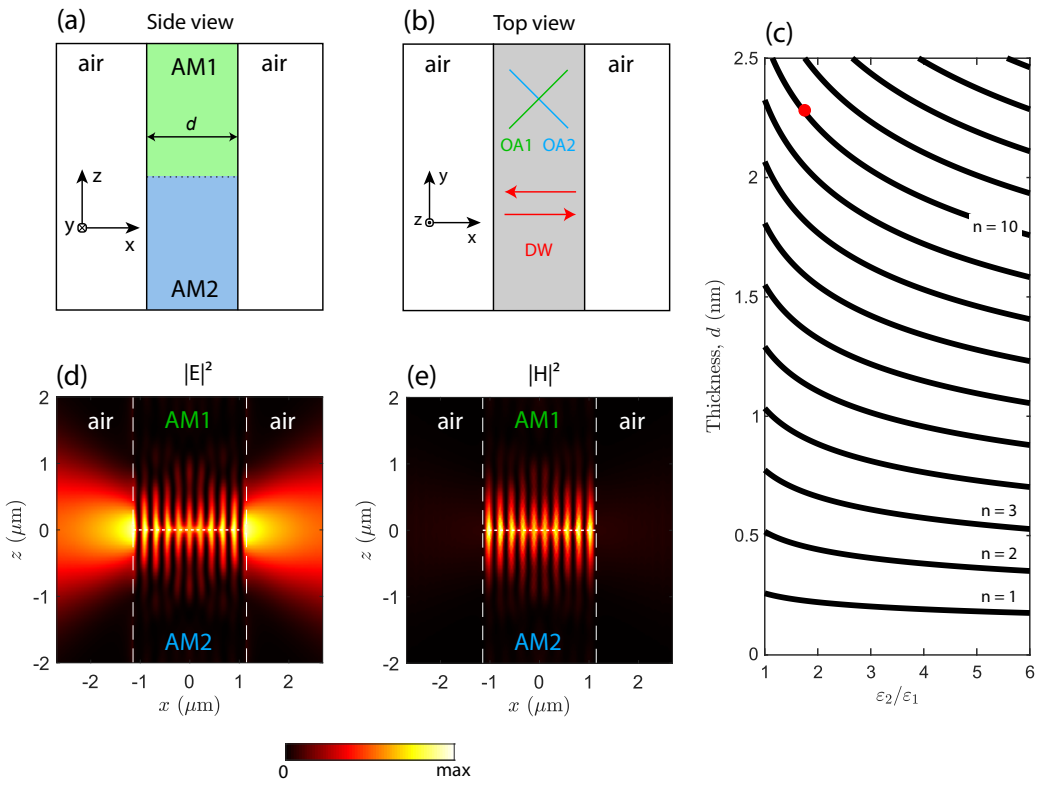

Figure 1: (Color online) Side view (a) and top view (b) of the interface between two anisotropic materials bounded by air from left and right. Optical axes of anisotropic materials are perpendicular to each other and form the angle of 45° to y-axis as shown by by green and blue lines in panel (b). Dyakonov-like mode in such confuguration is superposition of Dyakonov waves reflecting from both sides of the boundary at the angle of $\alpha = 0°$ as is shown in panel (b) by red arrows. Corresponding Fabry-Perot resonances calculated by Eq. (11) are shown in panel (c). Intensity of electric (d) and magnetic (e) fields of Dyakonov-like mode in such configuration. Colorscale is shown onthe right.

3 One-dimensional confinement at $\alpha = 45°$

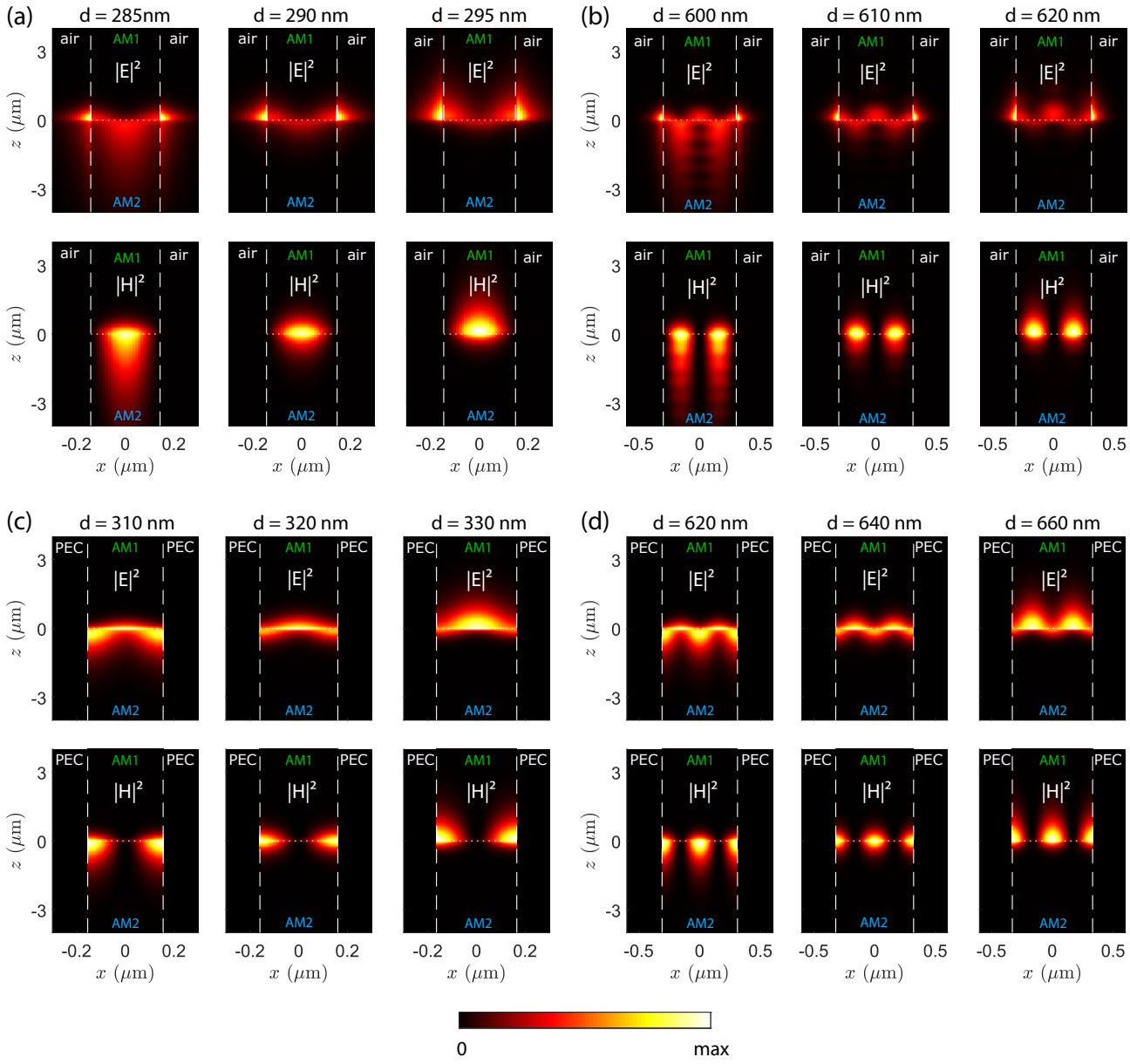

Figure 2: Electric and magnetic fields intensity profiles of DSWMs calculated for air and PEC boundaries for different waveguide widths d. Colorscale is shown on the bottom.

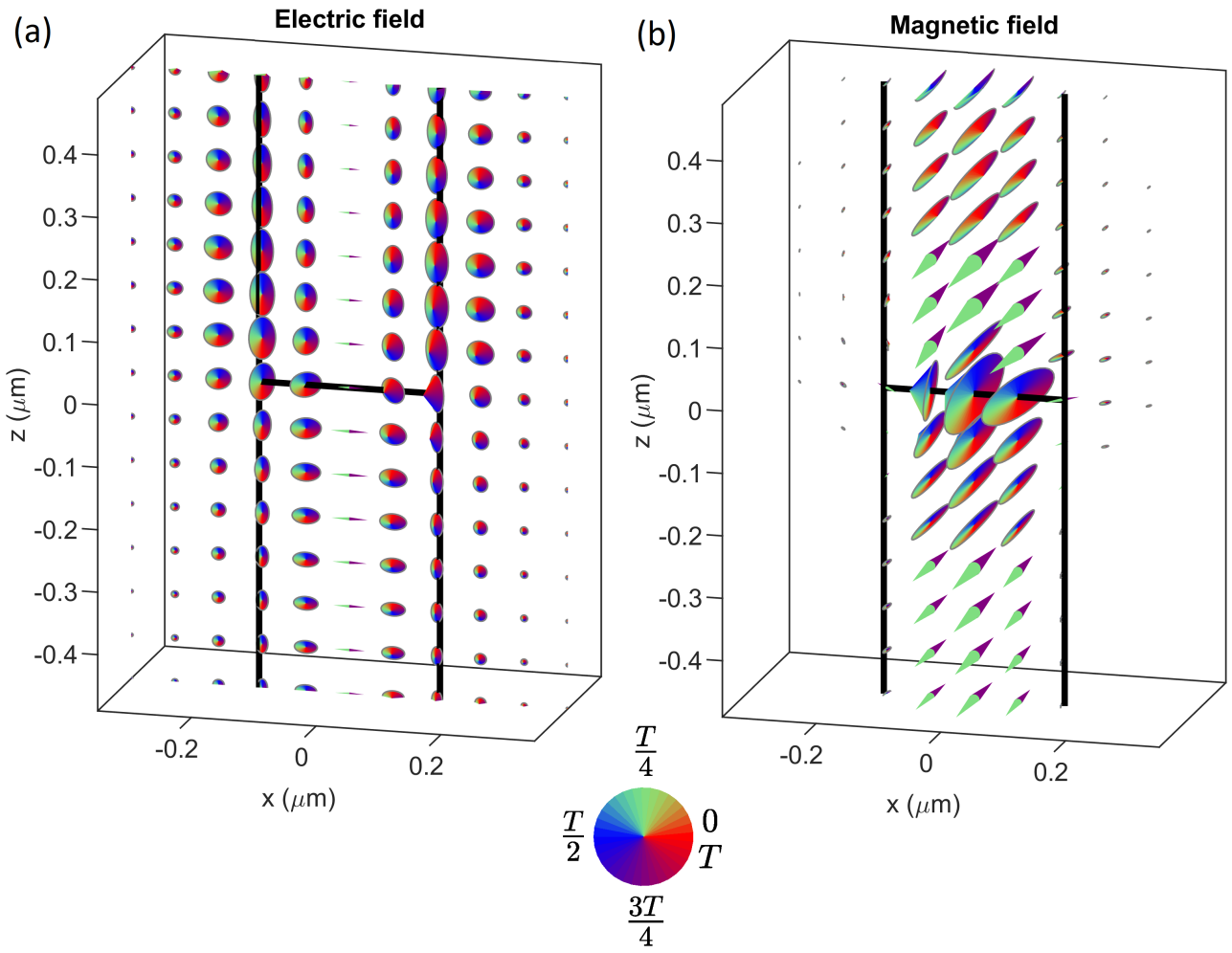

Figure 3: Electric (a) and magnetic (b) fields of DSWM in phase representation calculated for $\varepsilon_2 = 16$, $\varepsilon_1 = 9$, $\lambda = 1550\,\text{nm}$, $d = 290\,\text{nm}$, $k_x = 0$, $k_y = 2.7358(1/d)$. In the phase representation, we intend to show the field orientations during the entire period of electromagnetic oscillations. In such representation i) the cone base lies in the polarization plane where the field oscillates; ii) in the most general case, the cone base is an ellipse which is circumscribed by the field vector during one oscillating period. In the case of a linear polarization the ellipse degenerates into a straight line, while in the case of purely circular polarization, the ellipse degenerates into a circle; iii) the cone height is equal to the product of the electric field amplitude and the circular polarization degree; iv) the direction of the cone follows right screw rule; v) the color scale represents the phase of electromagnetic oscillations as explained on the bottom. See Ref. [1] for details.

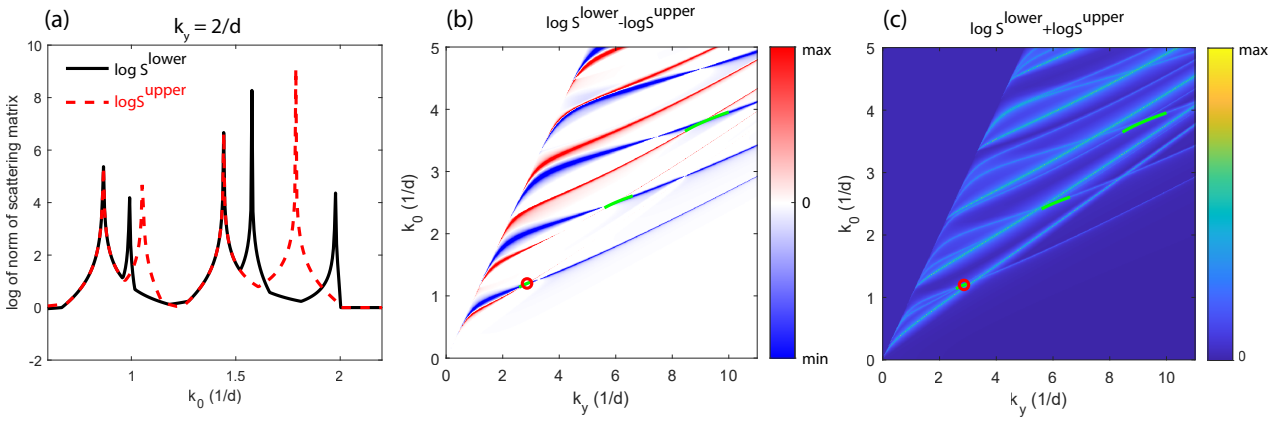

Figure 4: (a) k_0-dependence of the norm of the scattering matrix of the upper and lower slabs showing the spectral position of the waveguide modes at $k_x = 0$ and $k_y = 2/d$. One can see the common peaks for both slabs (ordinary waveguide modes) and the peaks existing only in one of the slabs (extraordinary waveguide modes). (b) $\log(S_{(lower)}) - \log(S_{(upper)})$ is a function of k_0 and k_y. Red and blue regions denote positive and negative values which correspond to the extraordinary waveguide modes of the upper and lower slabs. Green lines show Dyakonov surface waveguide modes (DSWM). One can see that the DSWM appear near the intersection of the upper and lower slabs' waveguide modes like in the case of the PEC boundary shown in the main text. (c) $\log(S_{(lower)}) + \log(S_{(upper)})$ is a function of k_0 and k_y showing the dispersion of both ordinary and extraordinary waveguide modes of the upper and lower slabs.

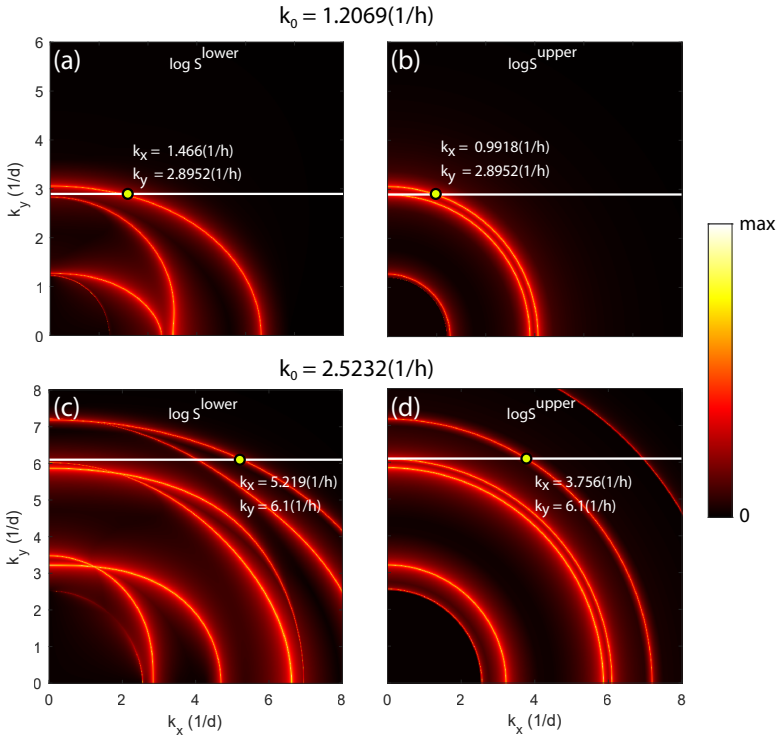

Figure 5: k_x and k_y dependencies of the norm of scattering matrix of the upper(b,d) and lower slabs (a,c) calculated at photon energies corresponding to the 1-st order ($k_0 = 1.2069/d$) and 2-nd order ($k_0 = 2.5232/d$) DSWMs. Reddish regions of large norm of scattering matrix indicate the positions of the upper and lower slabs' waveguide modes. On the waveguide modes dispersion curves, a specific waveguide mode is chosen (shown by a yellow dot) such that $k_y^{WG} = k_y^{DSWM}$ at a given photon energy of DSWM. DSWM with this energy can out-couple its energy to the selected waveguide mode if they have non-vanishing overlap integral. Colorscale is shown on the right.

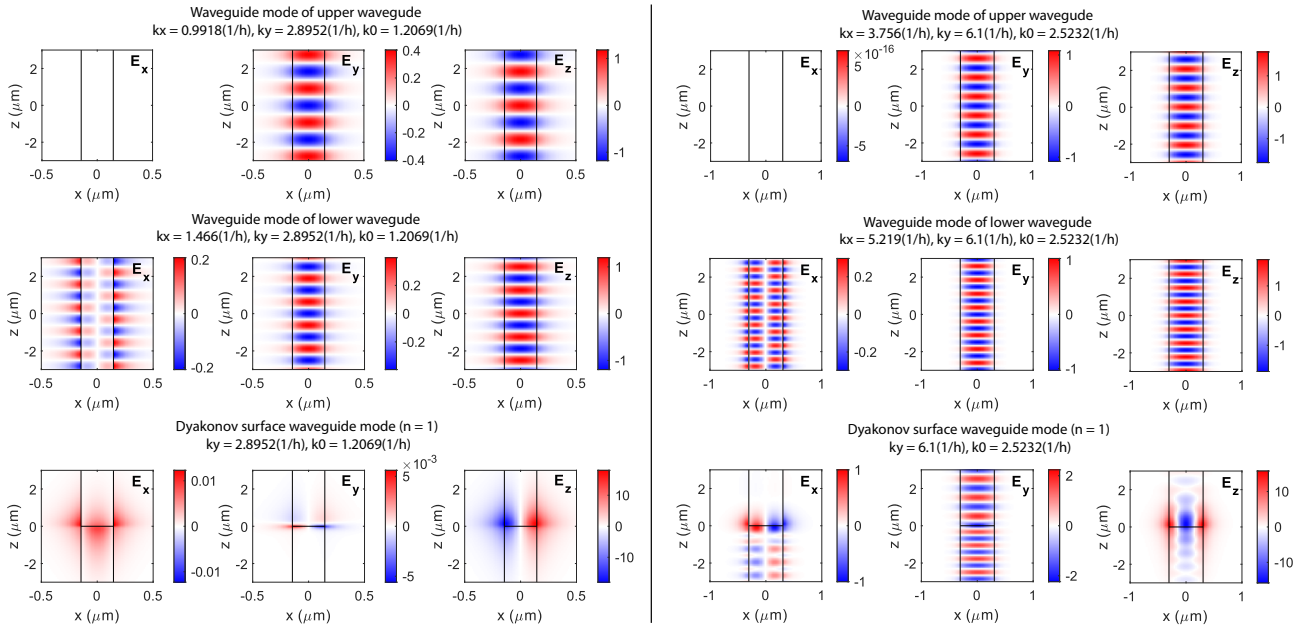

Figure 6: x-, y- and z-projections of electric field of upper slab's waveguide mode, lower slab's waveguide mode and DSWM calculate for the photon energies of the 1-st order DSWM (left panel) and 2-nd oder DSWM (right panel). Values of k_x, k_y and k_0 are specified in the titles. By comparing symmetries of the waveguide modes and the DSWMs, one can see that the 1-st order DSCM cannot couple to the waveguide modes.

4 Two-dimensional confinement

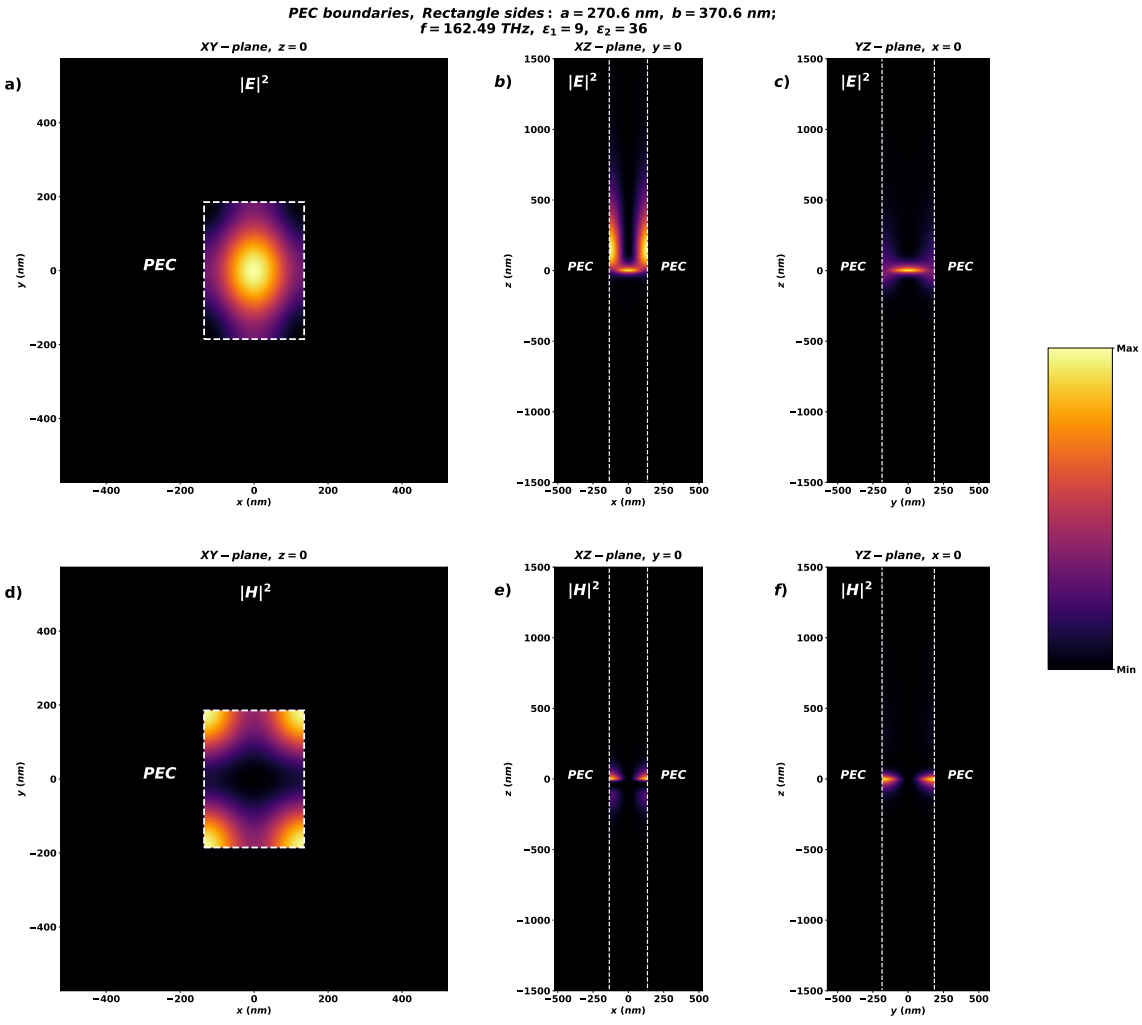

Figure 7: Electric and magnetic field intensity profiles of DSCM in horizontal cross-section $z = 0$ and two vertical cross-sections $x = 0$ and $y = 0$ in a rectangle cylinder with sides: $a = 270.6$ nm, $b = 370.6$ nm, and PEC boundaries. All simulations are made for $\epsilon_1 = 9$ and $\epsilon_2 = 36$.

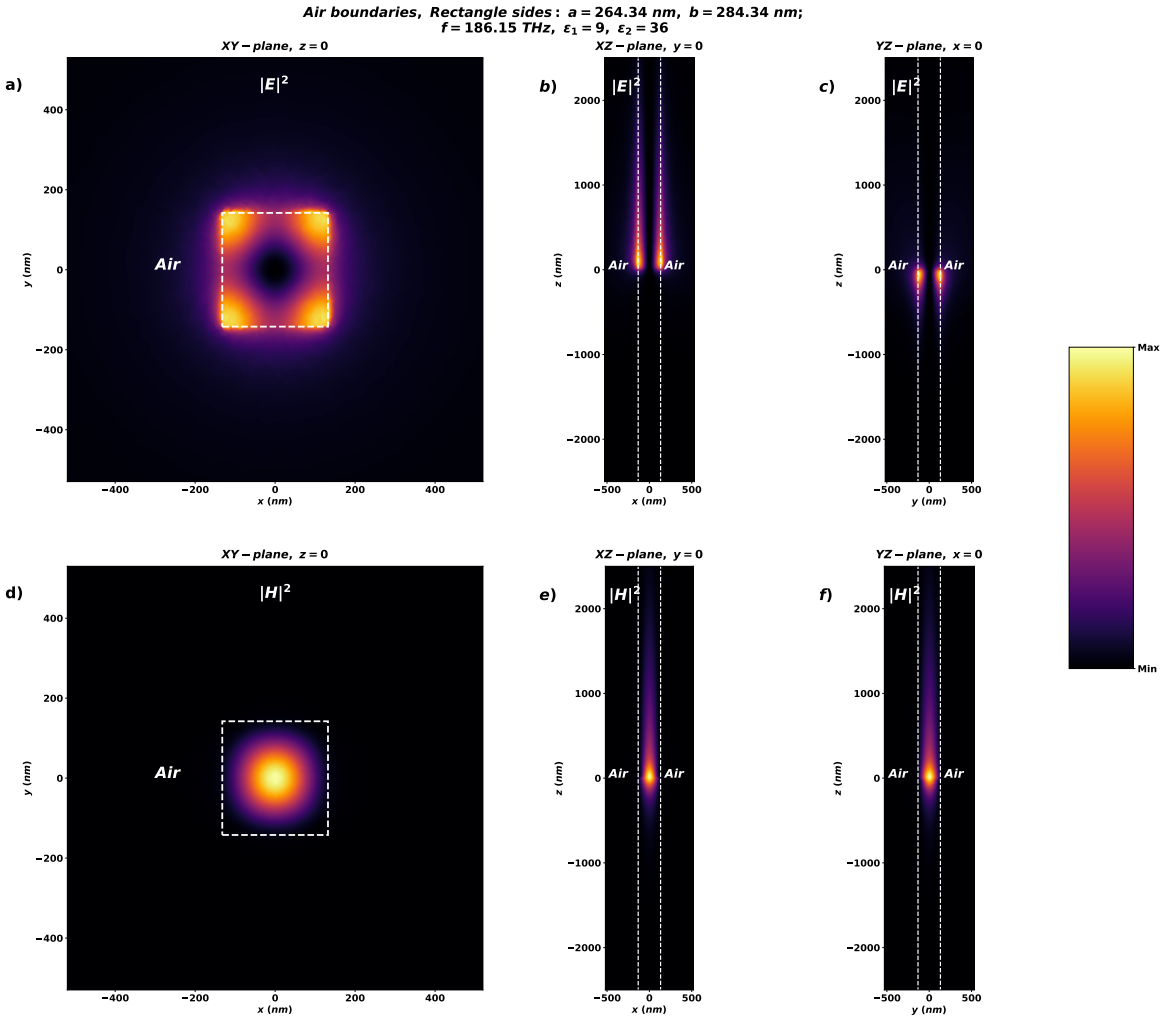

Figure 8: Electric and magnetic field intensity profiles of DSCM in horizontal cross-section $z = 0$ and two vertical cross-sections $x = 0$ and $y = 0$ in a rectangle cylinder with sides: $a = 264.34$ nm, $b = 384.34$ nm, and air boundaries. All simulations are made for $\epsilon_1 = 9$ and $\epsilon_2 = 36$.

References

[1] S. A. Dyakov, V. A. Semenenko, N. A. Gippius, and S. G. Tikhodeev. Magnetic field free circularly polarized thermal emission from a chiral metasurface. *Physical Review B*, 98(23):235416, 2018.